Molecular dynamics simulation of atomic-scale friction

R. Komanduri* and N. Chandrasekaran
Mechanical & Aerospace Engineering, Oklahoma State University, Stillwater, Oklahoma 74078

L. M. Raff
Chemistry Department, Oklahoma State University, Stillwater, Oklahoma 74078
(Received 23 April 1999; revised manuscript received 5 October 1999)

Molecular dynamics simulations of nanoindentation followed by nanoscratching were conducted on single crystal aluminum (with the crystal set up in the (001) [100] orientation and scratching performed in the [100] direction) at extremely fine scratch depths (from 0.8 nm to almost zero) to investigate the atomic-scale friction. The friction coefficients at these depths were found to be rather high (~0.6), nearly constant, and independent of scratch depth except for zero depth when the magnitudes of the forces were extremely small. The high values of the friction coefficient even at these fine scratch depths are attributed to the finite value of the scratch force involved in breaking and reforming of the atomic bonds, the high negative rake angle generally presented by the indenter (in the present case $-45°$) at fine scratch depths, which results in higher normal force (about twice the scratch force), and the absence of any lubricating film or contaminant between the sliding surfaces. The friction coefficient was also found to be close to the mean grinding coefficient, which is the ratio of the cutting to the thrust force with a high negative rake tool. Consequently, it appears that whenever material removal is involved in atomic-scale friction even at extremely fine scratch depths, the magnitude of the friction coefficient can be high, dependent on the rake angle presented by the tool, and independent of the normal force. This is because the magnitude of both normal and scratch forces increases with an increase in scratch depth and negative rake angle. Both the scratch hardness and indentation hardness were found to increase with decreasing scratch/indentation depth, strongly suggesting a size effect at fine scratch depths.

I. INTRODUCTION

Magnetic hard disks (usually made of aluminum) are used extensively in information storage systems. They are generally finished very rapidly and very efficiently by ultraprecision machining using single-point diamond tools on an expensive, highly rigid, high-precision machine tool. As the demand for higher storage space increases, the distance between the magnetic disk and the slider is being reduced significantly to nanometric dimensions (1–10 nm). Wear of the disk will further reduce this distance. As a result, the possibility of contact between the head and the disk resulting in adhesion, asperity contact, friction, and wear is increased significantly.[1–3] This will especially be the case if the lubricant fails. Also, sliders having extremely small mass (<10 mg) and very light contact loads (<1 μN) are being considered for ultrahigh-density recording devices using the point-recording technique.[4] A similar situation applies for microelectromechanical systems and ultrahigh-density recordings. Friction and wear under these conditions are believed to be due to surface interaction forces at the atomic level rather than the load[5] because of light loads and extremely light weights of the sliders. It appears that the traditional macroscopic theories of friction cannot be extended under these conditions.

The ultimate goal of nanotribology is to design practically zero wear devices with very small mass and extremely light loads.[2–5] Fundamental atomic-scale friction studies are anticipated to throw light on the nature of the friction process, the magnitudes of the friction force as well as the friction coefficient, and ultimately the relation between friction and wear, if any. Is the friction coefficient, low or high, under nanotribological conditions? What is its magnitude? What is its significance? Is it dependent on the normal load? Answers to these and other questions are important in pursuance of our knowledge in nanotribology. Understanding the science of nanotribology, therefore, is not only an intellectual curiosity but a definite technological need. The fact that a lubricating layer is provided between the disk and the read/write head (slider) to reduce friction and wear is an indication that without that, the friction coefficient is anticipated to be high. However, some experimental studies using atomic-force microscope and other devices report rather low friction values.[6,7] Of course, these studies may involve the introduction of a low friction coefficient lubricant either intentionally or formed *in situ* with the environment.

Nanotribology involves dynamic atomic interactions at the interface of two materials in relative contact. This includes adhesion, contact formation, nanoindentation, scratching, nanocutting, friction, wear, and lubrication.[2–4] Considerable research has been focused on the macroscopic, microscopic, and atomistic behavior of friction. Oftentimes, the microscopic and atomic behavior are combined into nanometric behavior. A number of theories such as the surface roughness theory,[8] the adhesion theory,[9,10] the delamination theory,[11] and friction due to molecular interactions[12–14] have been put forward to explain the origin of friction. However, surface roughness theories fail to explain energy dissipation and adhesion theories assume friction *a priori*. Other mechanisms, such as phonon interactions[15] and electron excitation,[16] have also been suggested. Theories explaining the dependence of the friction coefficient on such extrinsic

factors as surface roughness,[17–20] load,[20–24] sliding speed,[19–21,25] and hardness[26] have also been proposed. However, significant discrepancies exist on the nature and magnitude of the friction coefficient and its dependence on the extrinsic factors.

In the field of tribology, the coefficient of friction is considered as an important characteristic that can provide a significant insight into the frictional behavior of two contacting surfaces. Unfortunately, a wide range of friction coefficient values varying from extremely low (0.005),[6] to intermediate values of ~0.13,[27] to high values of 1.2 (Ref. 28) and 5 (Ref. 29) have been reported in the literature. Consequently, there is a genuine concern whether atomic-scale friction differs significantly from the macroscopic or even microscopic friction. Consequently, it is important to investigate the nature of atomic-scale friction in an attempt to provide a plausible explanation for the discrepancies in the magnitude of friction coefficient values observed by various researchers.

On the experimental side, atomic force microscopy (AFM) and scanning tunneling microscopy (STM), introduced a decade or so ago following the pioneering work of Binnig *et al.* in 1982,[30] are used extensively to investigate tribological interactions, such as adhesion, contact formation, friction, wear, microindentation, etc.[3–7] Mate *et al.*[6] conducted pioneering atomic-scale friction studies of a tungsten tip on graphite in the load range of 1 μN using an AFM in ambient air. They discovered that as the tip slides over the graphite surface, which has a hexagonal periodic arrangement of surface atoms, the tip experienced a periodic friction force with the same periodicity as the graphite structure thus relating for the first time the friction force variations with the atomic structure of one of the sliding elements. They reported the friction coefficient to be extremely low and in the range of 0.005–0.015, depending on the tip geometry. Erlandsson *et al.*[7] extended the friction studies of a tungsten tip on a muscovite mica and found similar results. Analogous to the graphite-tungsten combination, they found the friction force to vary with the same periodicity as the hexagonal layers of SiO_4 units that form the cleavage planes of mica. They estimated the average friction coefficient to be ~0.09. Skinner, Gane, and Tabor[31] also reported extremely low friction coefficients (0.005–0.02) for a tungsten tip sliding on graphite surface in vacuum for loads in the range of 10–400 μN. They considered at length the origin of the frictional force in the case of a tungsten stylus sliding on the basal plane of graphite with little or no deformation. Flaking of graphite was discounted as a possible mechanism for friction at low loads as flaking is produced by a cleavage mechanism and not friction. They also pointed out that plastic deformation or shear is not observed in their experiments. Based on these observations, they proposed that the chief component of friction arises from an adhesion-type mechanism at the stylus/graphite interface. This is very similar to Kaneko's suggestion that friction and wear at extremely light loads are due to surface interaction forces at the atomic level rather than the load.[5]

It may be noted that the use of the scanning probe microscopes, such as AFM and STM, involves significant cost, time, and technological constraints. Also, the results can be influenced by such extrinsic factors as surface contaminants, surface state, geometry of the slider, depth of sliding, etc. Molecular dynamics (MD) simulation, which can also be used for investigating atomic-scale phenomenon, is a viable alternative for the study of the atomic-scale friction process. To simulate sliding at extremely small depths (in the order of nm), MD simulations of nanoindentation followed by nanoscratching were conducted in this investigation on a single crystal aluminum [with (001)[100] combination of crystal orientation and [100] direction of scratching] at extremely fine scratch depths (0.8 nm to almost zero). Values of the scratch force (or friction force), the normal force, the resultant force, the specific energy (energy required for removing unit volume of material), the friction coefficient, the indentation hardness, and the scratch hardness for various scratch depths were determined. It may be pointed out that MD simulations of the indentation process have been reported in significant detail in the literature.[32–37] The emphasis of the current investigation is not on the details of the indentation/scratching process but to study the atomic-scale friction involving the friction coefficient at extremely fine scratch depths reaching almost to zero depth. Further, unlike in the experimental work involving scanning probe microscopes, such as AFM and STM, where the results are influenced by the stiffness of the system, in the MD simulation, it is possible to investigate the atomic-scale friction independent of the system characteristics. Although MD simulations offer many advantages, it is important to bear in mind that the interaction potentials used in such studies are, at best, only modestly accurate approximations to the true system potential. It is, therefore, important to determine the sensitivity of the conclusions drawn from these simulations to reasonable variations of the potential parameters. It is also necessary to employ high cutting and/or sliding velocities to keep the computational requirements of the study within acceptable limits. Because of this, appropriate caution needs to be exercised in data interpretation. Alternatively, the number of atoms under consideration and, consequently, the computational time can be reduced significantly by maintaining the length of the work material being cut at a constant, as originally proposed by Belak, Boercker, and Stowers.[38] In this technique, the atoms in the work material after the tool passes are discarded and new atoms are added at the other end of the work material. This work was followed by Chandrasekaran *et al.*[39]

It may be noted that in the case of friction experiments involving scratching, the two forces involved are the scratch force and the normal force. The equivalent terms in cutting, grinding, etc., are the cutting (or the grinding) force and the thrust force, respectively.

II. PREVIOUS MD SIMULATION STUDIES OF ATOMIC-SCALE FRICTION

The variation of the friction coefficient with load suggests the dependence of the mechanism of friction on the scale of interaction.[40] Hence, it is necessary to understand the mechanism of friction and the dependence of the friction coefficient on extrinsic and intrinsic factors at the atomic level. Landman, Luedtke, and Ribarsky[41] conducted MD simulation of two contacting solids to evaluate the critical shear stress. The failure was reported to take place along the weakest plane of the softer material. In contrast to the low friction coefficients

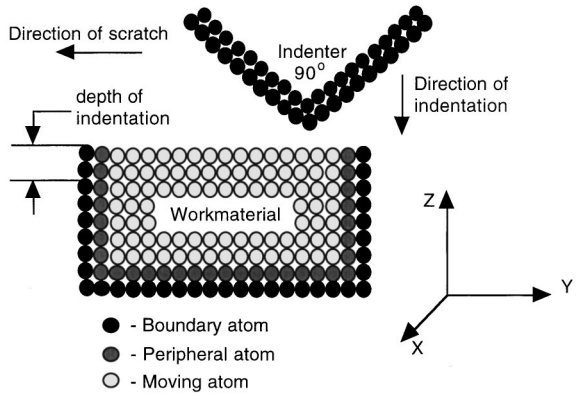

FIG. 1. Schematic of the indentation/sliding model used in the MD simulations showing various regions of interest, namely, the moving zone, the peripheral zone, and the boundary zone.

(0.005–0.015) reported using AFM,[6,7] Landman, Luedtke, and Ribarsky report friction coefficient values in the range of 0.77. Buldum and Ciraci[42] conducted MD simulation of nanoindentation and sliding of a Ni tip on a Cu substrate, with a sharp Ni (111) tool on a Cu (110) surface and a blunt Ni (001) tip on a Cu (001) surface. An embedded-atom potential was used to simulate the metallic bonds of Ni and Cu. A quasiperiodic variation in the force was reported during sliding of the sharp Ni tip on the Cu substrate. This was attributed to the stick-slip process involving phase transitions. Accordingly, one layer of the asperity deforms and matches the substrate during the first slip followed by two asperity layers merging into one through structural transition during the second slip. The ratio of the static to kinetic friction force was reported to be ~2.

Komanduri, Chandrasekaran, and Raff[43] conducted MD simulations of indentation/scratching on different crystallographic planes and directions of scratching to study the anisotropy in hardness and friction coefficient of single crystal aluminum at a constant scratch depth of 0.8 nm. They reported friction coefficient values in the range of 0.6–0.9 with the maximum along (001) $[\bar{1}10]$ and the minimum along (110) $[\bar{1}10]$. The value of the friction coefficient along (001) [100] was reported to be 0.698. However, it was not clear from that study whether the friction coefficient would remain the same or decrease with decrease in scratch depth ultimately reaching to zero scratch depth values. This investigation was specifically undertaken at extremely low scratch depths with that objective in mind. In a related investigation involving nanometric cutting of single crystal aluminum in various crystal orientations and directions of cutting, Komanduri, Chandrasekaran, and Raff[44] reported anisotropy in forces and specific energy in the range of 29%, which is close to the value of its anisotropy in the elastic range (21.9%).[45] A similar situation can exist for the dependence of friction on crystallographic orientations although this has not yet been investigated.

Kim and Suh[40] conducted MD simulations of friction for a single atom sliding nondestructively over a triangular surface with a two-dimensional (2D) Lennard-Jones potential and a specified normal force. The normal force was kept very low to avoid mechanical interactions such as plowing, asperity deformation, etc. The interfacial interaction was kept strictly repulsive based on the justification that the repulsive forces are short-range forces and primarily responsible for supporting loads at the point of contact between two solids under applied force. In the case of static simulations, a periodic oscillation of the tangential force and the normal force as the atom scans the lattice was reported. The friction coefficient was observed to oscillate between -0.8 and 0.8 for a case when the scan height was $1.1a$, where a is the lattice parameter of the surface. In the case of constant force simulations at similar scan height, the friction coefficient was reported to vary between -1.0 and 1.0. Average friction coefficients of ~0.05 were reported for elastic interaction between the atom sliding over the work surface. Of course, this value would be much higher had they considered plastic interactions as is the case with atomic-scale friction involving material removal.

Shimizu *et al.*[29] conducted MD simulation of friction of a rigid diamondlike tool on a single crystal copper in the (111) plane at 1 m/s to investigate stick-slip phenomena such as those observed using an AFM. A Morse potential was used for the copper atoms and an interaction potential proposed by Inamura and Takezawa[46] was used between copper and diamond atoms. It may be noted that no diamond potential is actually used in this case. Instead an infinitely hard indenter

TABLE I. Morse potential parameters for some of the fcc and bcc metals (Ref. 48).

Metal	Crystal structure	Lattice constant (Å)	α parameter ($Å^{-1}$)	Equilibrium radius γ_e (Å)	D parameter (eV)
Lead	fcc	4.95	1.1836	3.733	0.2348
Aluminum	fcc	4.05	1.1646	3.253	0.2703
Silver	fcc	4.09	1.3690	3.115	0.3323
Copper	fcc	3.62	1.3588	2.866	0.3429
Nickel	fcc	3.52	1.4199	2.780	0.4205
Iron	bcc	2.87	1.3885	2.845	0.4174
Chromium	bcc	2.89	1.5721	2.754	0.4414
Molybdenum	bcc	3.14	1.5079	2.976	0.8032
Tungsten	bcc	3.165	1.4116	3.032	0.9906

TABLE II. Computational parameters used in the MD simulation of indentation/scratch.

Configuration	3D indentation scratch
Work material	Aluminum
Crystal structure	fcc
Lattice constant	4.05 (Å)
Potential used	Morse potential parameters used: $D=0.2703$ eV, $\alpha=1.1646$ Å^{-1}, $r_0=3.253$ Å
Work material dimensions	$6a\times25a\times15a$, a-lattice constant
Indenter dimensions	$6a\times15a\times15a$, a-lattice constant
Indenter material	Infinitely hard
Indenter edge radius	Sharp edge
Indenter rake angle	$-45°$
Indenter included angle	90°
Indentation/scratch depth	0.8–0.1 nm, sliding slightly below the surface, and on the surface
Width of scratch	2.12 nm
Indentation/scratch speed	500 m/sec
Bulk temperature	293 K

was considered. They confirmed the atomic-scale stick-slip phenomenon in friction. They also reported the average friction coefficients to vary from ~0.5 to 5 while the maximum friction coefficient varied from ~4 to 19 depending on the spring constant (5–100 N/m) and spring force (0.1–0.6) of the system used.

III. METHODOLOGY FOR MD SIMULATION OF INDENTATION/SLIDING

A. Indentation/Sliding model of MD simulation

Figure 1 is a schematic of the indentation sliding model used in the MD simulation. The work material is divided into

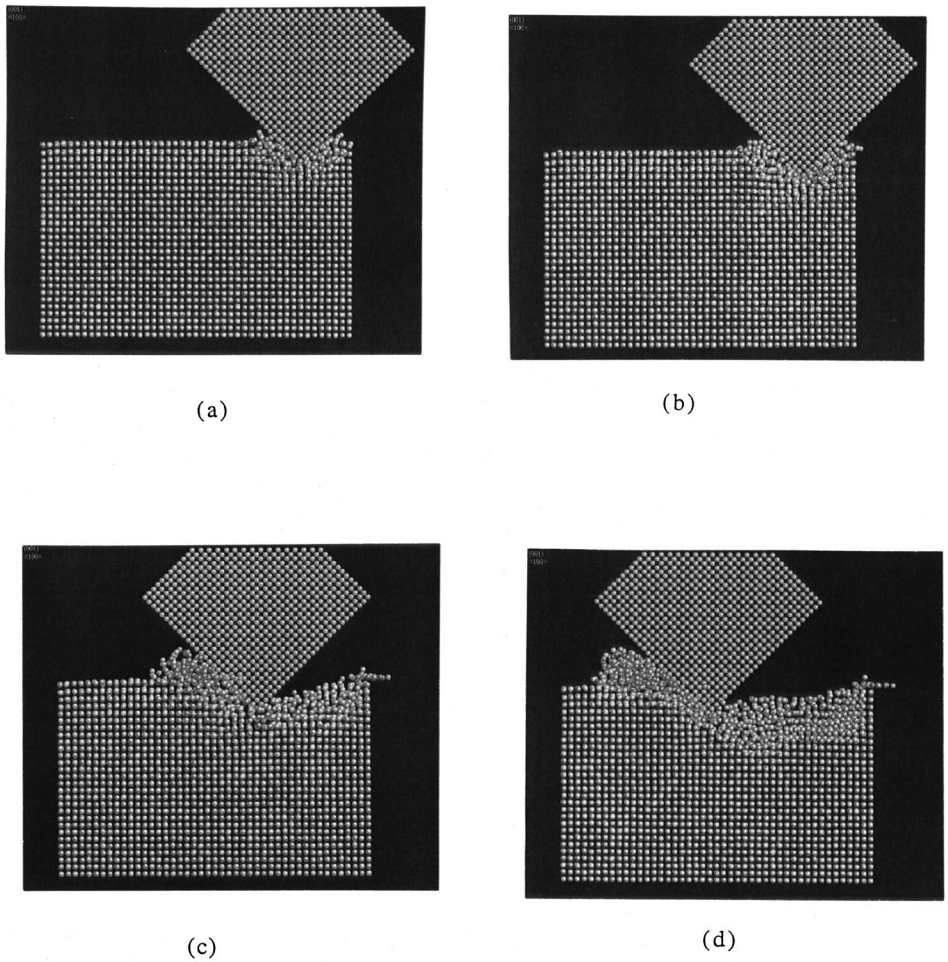

FIG. 2. MD simulation plots showing various stages of the scratch process at a scratch depth of 0.8 nm.

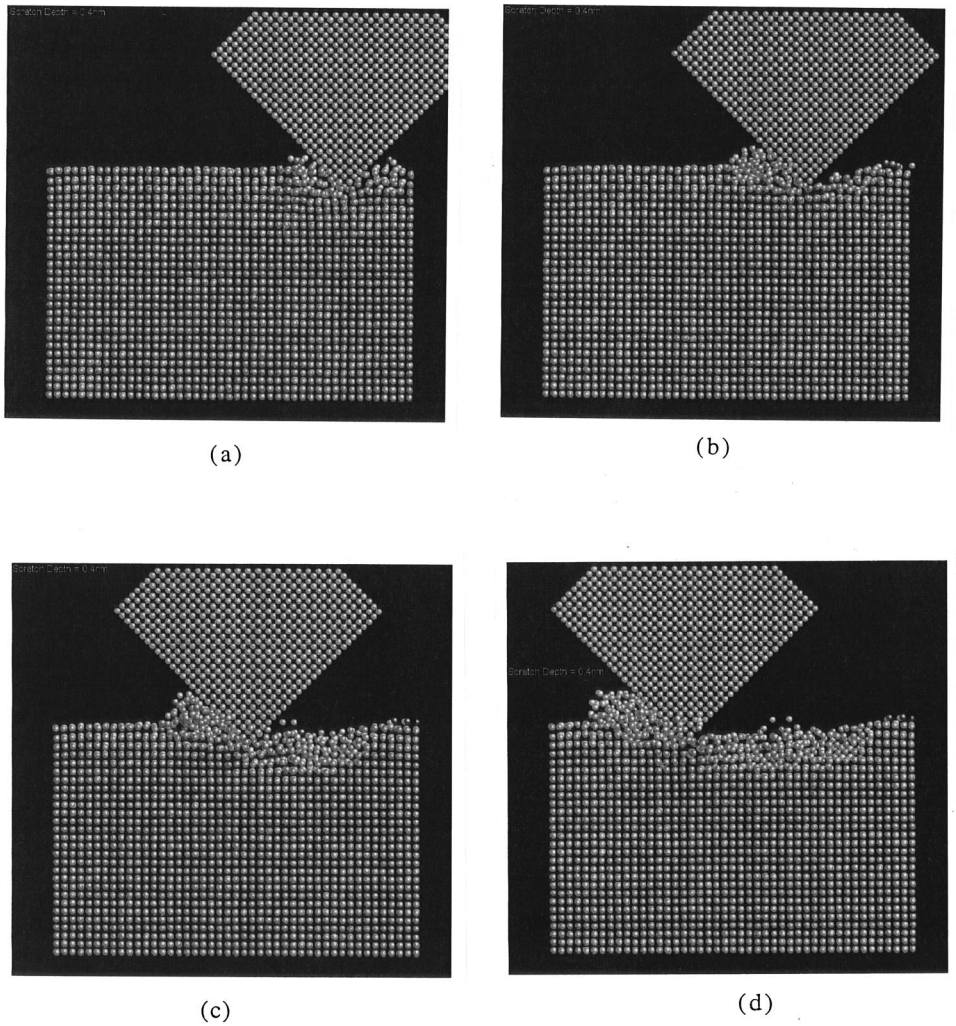

FIG. 3. MD simulation plots showing various stages of the scratch process at a scratch depth of 0.4 nm.

three different zones, namely, the moving zone (P zone), the peripheral zone (Q zone), and the boundary zone (B zone).[47] The motions of the atoms in the moving zone are determined solely by the forces produced by the interaction potential and the direct solution of classical Hamiltonian equations of motion. The motions of the peripheral atoms are also calculated from the solution of Hamiltonian equations but modified by the presence of velocity reset functions associated with each atom in the peripheral zone. The boundary atoms are fixed in position and serve to reduce the edge effects and maintain proper symmetry of the lattice. Details on this are given in Chandrasekaran *et al.*[39]

B. MD simulation conditions

MD simulations of nanoindentation/nanosliding were conducted on single crystal aluminum on a Digital α workstation (Model 500) with a clock speed of 500 MHz. In an earlier study, based on nanometric cutting on various crystal orientations and cutting directions, Komanduri, Chandrasekaran, and Raff[44] recommended that the (001) [100] combination be used for simulating machining/scratching, if only one orientation has to be used, as it represents conditions close to macroscale cutting of polycrystalline materials. Consequently, in this investigation, the crystal was setup with (001)[100] orientation and scratching performed along the [100] direction. For convenience, an infinitely hard (nickel) tool was used in these simulations as wear of the indenter is not considered. The empirical potential used for the simulation was a pairwise sum of Morse potentials:

$$V_{ij}=D\{\exp[-2\alpha(r_{ij}-r_e)]-2\exp[-\alpha(r_{ij}-r_e)]\},$$

where r_e and r_{ij} are equilibrium and instantaneous distances between atoms i and j, respectively. D and α are constants determined on the basis of the physical properties of the material. For example, r_e, α, and D are obtained from the closest spacing between the atoms (equilibrium lattice spacing), the Debye temperature, and the sublimation energy, respectively. Table I gives the parameters of the Morse potentials for some of the fcc and bcc metals after Girifalco and Weizer.[48] The validity of the function as well as the stability of the crystal for a given material is checked for various properties including cohesive energy, the lattice constant, the compressibility, and the elastic constants as well as the equation of state and stability of the crystal. It is always a question as to how well these parameters represent the system potential. For that, one can conduct sensitivity studies by varying the Morse parameters slightly, say $\pm 5\%$. However, one needs to be careful not to vary to such an extent that the potential approaches that for another metal. A case in point is aluminum and lead. If the D parameter of aluminum is re-

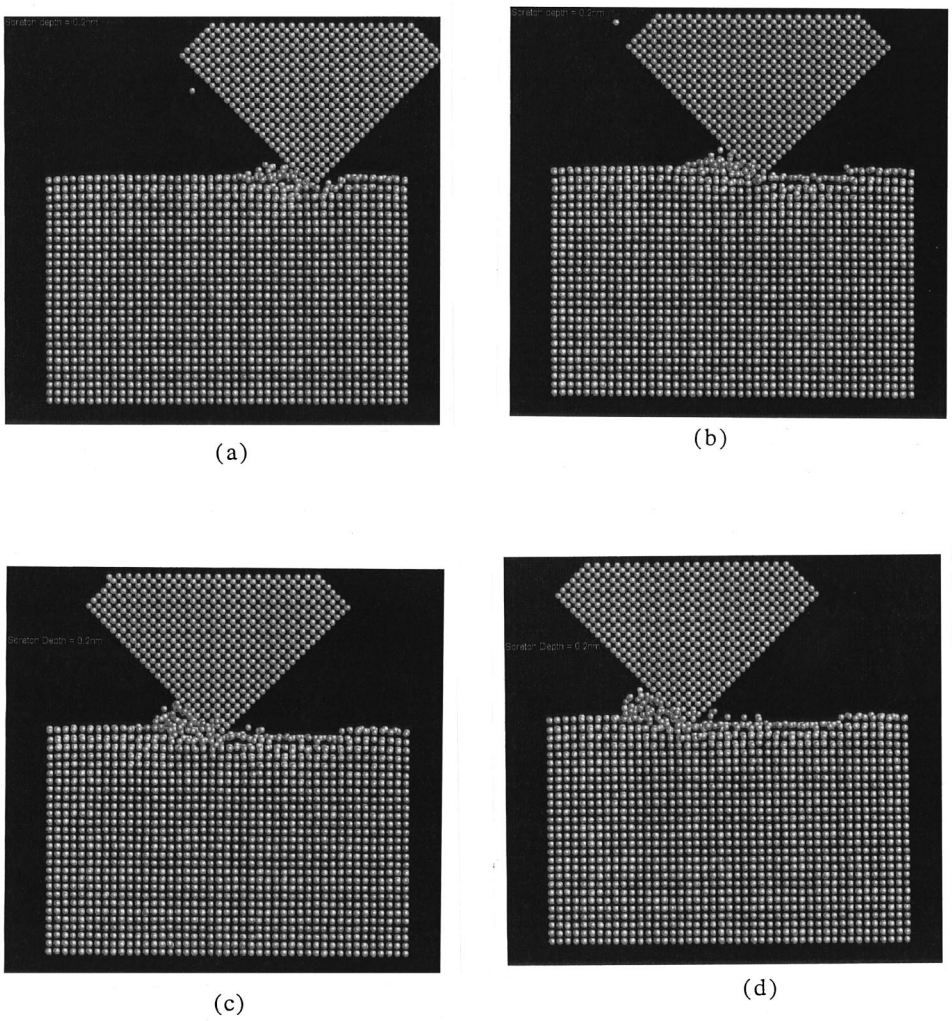

FIG. 4. MD simulation plots showing various stages of the scratch process at a scratch depth of 0.2 nm.

duced by 10%, the potential would represent lead more than aluminum as the other two parameters (α and r_0) are very close. In this investigation a sensitivity analysis is conducted for one depth of scratch (0.1 nm) by varying the most important of the Morse parameters, namely, the D parameter by $\pm 5\%$. Table II gives the computational parameters, details of the aluminum work material and tool dimensions, the indentation/scratch depth, and the length of slide used in the simulations.

IV. RESULTS

A. MD simulation results

In the following, MD simulation results of the indentation/sliding on a single crystal aluminum at extremely fine depths (0–0.8 nm) are presented. MD simulation plots at different stages of the process are given for a better appreciation of the process. It may be noted that the width of the tool in this investigation was taken as being equal to the width of the work material (perpendicular to the paper). The tool center coincides with the work material origin during the indentation/sliding process. Even though in practical cases the tool width is less than the work material width, this approach is used to facilitate observation of the deformation process more clearly than by having the tool width less than that of the work material. The discussion of the indentation/sliding process is based not only on the MD simulation plots but also on the detailed observation of the animations of the process.[49]

In the MD simulations, the indentation/scratch depth was reduced from 0.8 nm to practically zero (tool sliding on the surface) in steps. Even at nominally zero scratch depth, some contact between the tool and the work material and subsequent material removal was observed (as will be shown) due to relaxation of the atoms in the structure. This condition is termed here as sliding slightly below the surface. In order to simulate a zero scratch depth condition, the tool was initially set slightly above the work material so that after relaxation, the surface of the work material was just beneath the tool tip, i.e., touching but no removal. This situation is termed as sliding on the surface. For this reason, indentations were performed only in the depth range of 0.8–0.1 nm and not in the two special cases discussed above.

Figures 2(a)–2(d) to 7(a)–7(d) are MD simulation plots showing the initial and the final stages of the scratch process at various scratch depths (0.8–0.1 nm, sliding slightly below the surface, and sliding on the surface) showing the nature of deformation ahead of the indenter and material removal in the form of chips. Figures 2(a), 3(a), 4(a), and 5(a) are initial stages of the scratch process (after indentation) performed at 0.8, 0.4, 0.2, and 0.1 nm scratch depth, respectively. Figures 2(b)–2(d), 3(b)–3(d), 4(b)–4(d), and 5(b)–5(d) show subse-

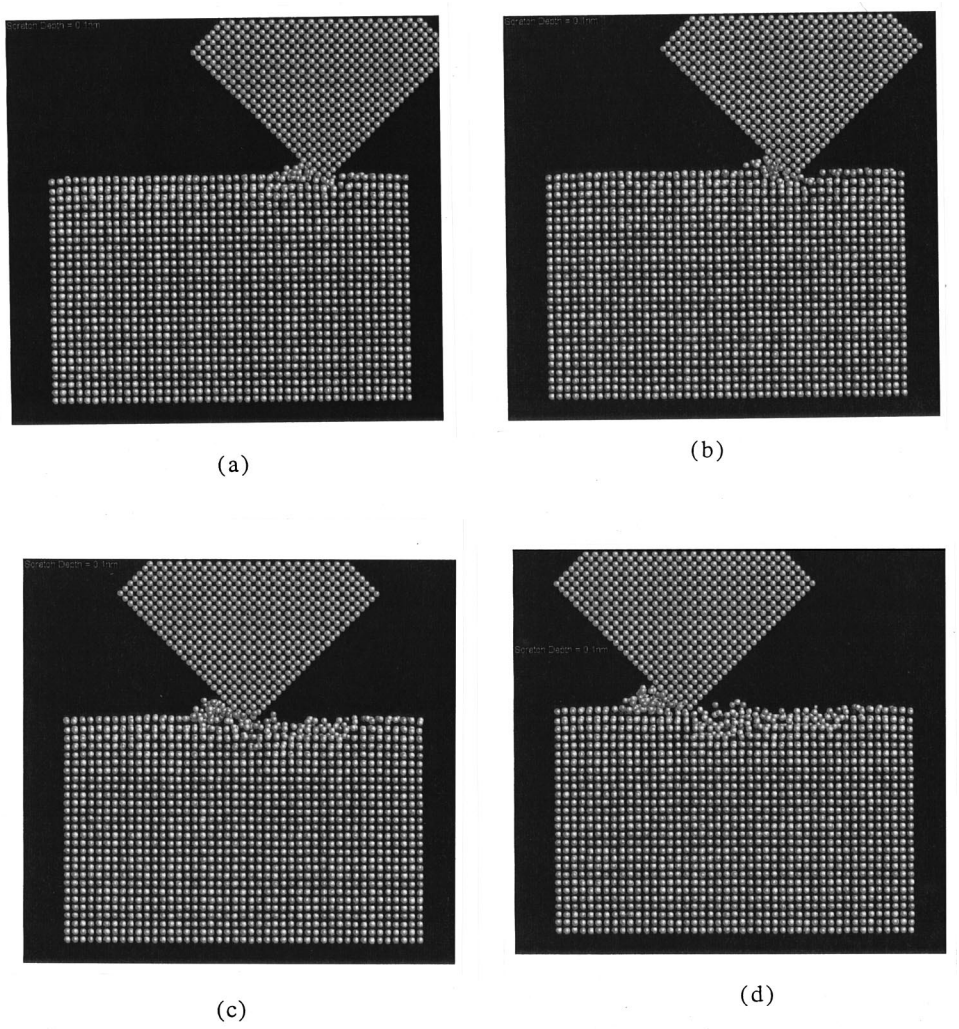

FIG. 5. MD simulation plots showing various stages of the scratch process at a scratch depth of 0.1 nm.

quent stages of scratching. They show the material removal taking place via the generation of chips as in conventional machining. However, due to the use of a high negative rake angle ($\sim 45°$) for the indenter, it can be likened more to plowing than cutting. The rake angle in cutting is the angle between the tool rake face and the normal to the cutting velocity vector. In the present case, it is the angle between the indenter face and the direction of scratching. Some subsurface deformation, estimated to be approximately equal to the indentation-scratch depth, especially at larger scratch depths, can also be seen. In the case of the tool sliding slightly below the surface, chip formation is not very prominent although a few atoms being removed from the top surface of the work material can be seen [Figs. 6(a)–6(d)]. Absence of material removal can be seen when the tool was slid on the surface of the work material without scratching [Figs. 7(a) and 7(d)].

B. On the nature of variation of the forces and energy

Figures 8(a)–8(f) are the force-displacement plots obtained in MD simulation of indentation/scratching at various depths (0.8 nm to almost zero). They are the raw data used in the analysis. Table III summarizes the results of the MD simulation giving the values of the scratch force, normal force, resultant force, specific energy, friction coefficient, indentation hardness, and scratch hardness for various scratch depths. In the cases where the tool was slid slightly below the surface and on the surface, the area of contact is practically zero. Consequently, the corresponding specific energy, indentation hardness, and scratch hardness values were not calculated as they may not be very meaningful.

In the following, the nature of the force-displacement curves [Figs. 8(a)–8(f)] is presented. The repulsive force is considered negative. During indentation, the normal force increases rapidly and the scratch force (tangential force) remains nearly zero. The increase in the repulsive force, though exhibiting minor fluctuations, is essentially uniform. After the indentation process, when the indenter was slid along the scratch direction, the normal force drops significantly. Further, during the scratch process, the primary force is along the scratch direction and hence the normal force drops significantly. As scratching proceeds, the scratching force increases while the normal force decreases [Figs. 8(a)–8(f)]. It can also be noted that the scratching force is lower than the normal force (also taken as the average values in Table III) as the indenter presents a high negative rake angle ($-45°$) during the sliding process. Once the indenter has moved through a specified scratch distance, it was retracted from the work material. The force corresponding to this segment of the simulation drops to zero as the tool-work separation increases. Hysteresis in the indentation-retraction curve can also be seen. In the cases of sliding slightly below

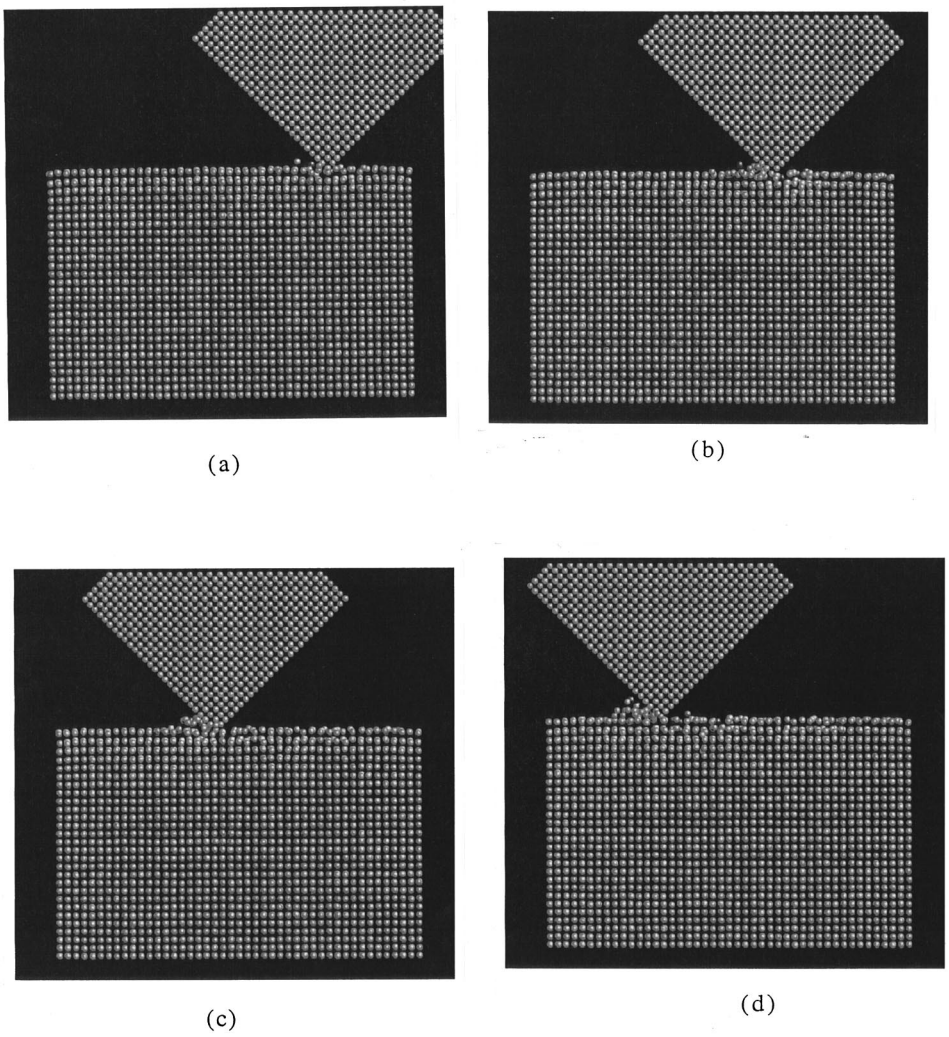

FIG. 6. MD simulation plots showing various stages of the scratch process in the case of the indenter sliding slightly below the surface of the work material.

the surface and on the surface, indentation was not performed. Consequently, Figs. 8(e) and 8(f) do not have indentation force trends. Even as the sliding depth is reduced from 0.8 to 0.1 nm, the position of the thrust-force curve with respect to the cutting-force curve seems to be constant. In other words, comparison of Figs. 8(a) to 8(e) suggests that the ratio of the cutting force to the thrust force is nearly constant as will be shown in the subsequent discussion. In the case of sliding on the surface both the forces seem to be close to zero [Fig. 8(f)].

In general, indentation tests are conducted at constant load. However, in the present investigation, a constant velocity condition is used instead, for convenience. Consequently, the indentation force is taken as the average of the forces during the entire indentation process. The indentation hardness of the work material is evaluated as the average force over the contact area of the indenter with the work material. The scratch hardness was calculated as the scratch force over the deformation supporting area of the indenter. The friction coefficient is evaluated as the ratio of the scratch force over the normal force, where the forces are the average values over the scratch length.

Figures 9(a)–9(c) show the variation of the scratching force, the normal force, the resultant force, the friction coefficient, and the specific energy during the scratch process for various scratch depths. Figure 9(a) is the variation of the scratching force, the normal force, and the resultant force with scratch depth. A depth of $\sim$0.05 nm is assumed in the case of the indenter sliding slightly below the surface. The force values in the case of the indenter sliding on the surface are plotted before the force values in the case of the indenter sliding slightly below the surface (0.05 nm). The forces can be observed to reduce with decreasing scratch depth. Both the scratch and the normal forces seem to follow a straight line relationship with scratch depth. Also, the normal force is higher than the scratch force in all the cases (except for sliding on the surface) suggesting that scratching is performed with a high negative rake tool. Figure 9(b) shows the variation of friction coefficient with scratch depth. Since the forces in the case of sliding on the surface were observed to be very close to zero (Table III), the friction coefficient value is not plotted for this case. It can be seen that the friction coefficient is nearly constant for various depths of scratching. Figure 9(c) shows the variation of specific energy with scratch depth, which shows an increasing trend with decreasing scratch depth. This can be attributed to the size effect similar to the ones reported by other researchers.[50–53]

Figure 10 shows the variation of the scratch hardness with scratch depth. The scratch hardness can be seen to increase with decreasing scratch depth. This increase is small as the depth is reduced from 0.8 to 0.4 nm. However, further re

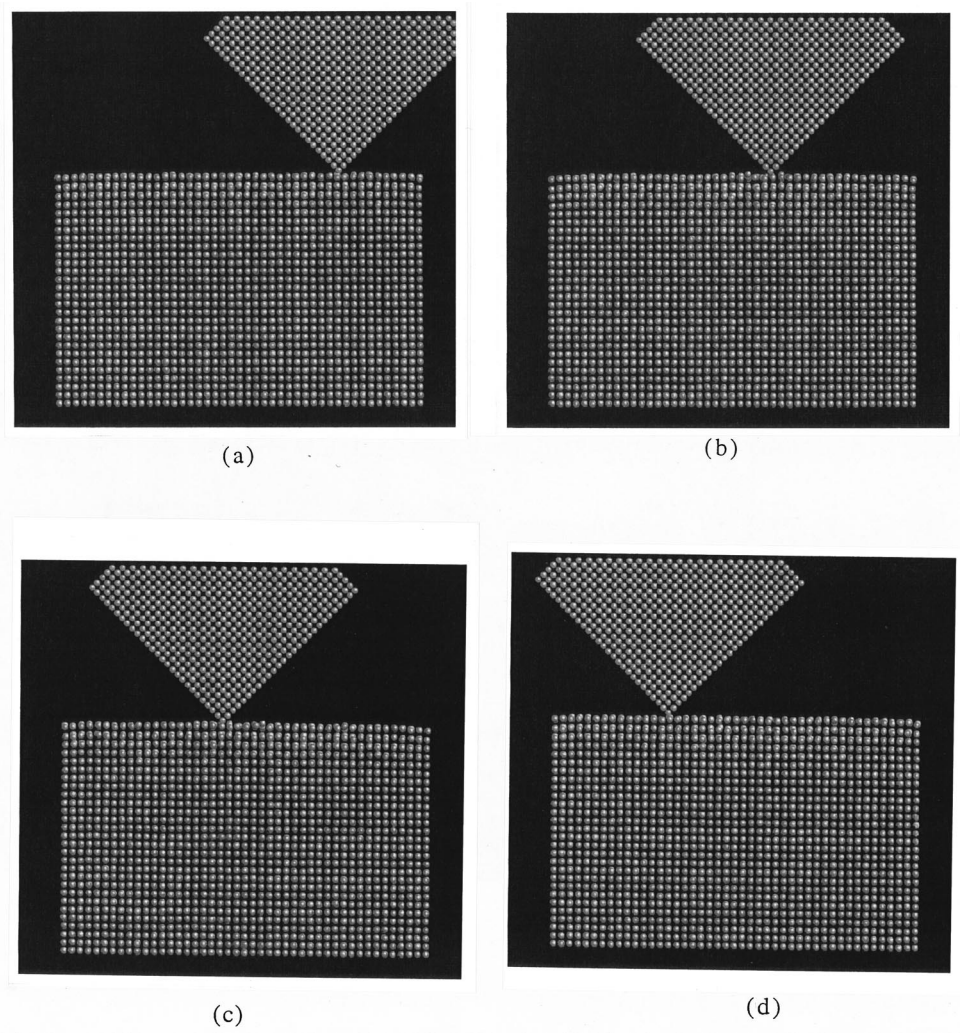

FIG. 7. MD simulation plots showing various stages of the scratch process in the case of the indenter sliding on the surface of the work material.

duction in the scratch depth results in a significant increase in the scratch hardness as shown in Fig. 10. Figure 11 shows the variation of indentation hardness with depth of indentation. At the extremely small indentation depths used in this study, an increase in indentation hardness with decreasing depth of indentation can be seen, again indicating a size effect.

C. Sensitivity of results due to variation in the *D* parameter of the Morse potential

Table IV summarizes the results of the sensivity analysis conducted for one depth of scratch (0.1 nm) by varying the most important of the Morse parameters, namely, the *D* pa-

TABLE III. Results of MD simulation study of nanoindentation sliding conducted on aluminum single crystals with (001)[100] orientation for different depths.

Depth of indentation-scratch (nm)	Scratch force/unit width (F_s) (10^2 N/mm)	Normal force/unit width (F_n) (10^2 N/mm)	Friction coefficient (F_s/F_n)	Resultant force/unit width (F_R) (10^2 N/mm)	Specific energy[a] (GPa)	Indentation hardness (GPa)	Scratch hardness (GPa)
0.8	1.485	2.127	0.698	2.594	18.3	5.068	21.360
0.4	0.741	1.148	0.645	1.366	18.3	5.460	23.074
0.2	0.443	0.724	0.612	0.878	21.9	5.930	30.486
0.1	0.337	0.510	0.661	0.611	33.3	5.871	40.974
Slightly below the surface	0.167	0.296	0.565	0.334			
Sliding on the surface	0.019	0.009	2.111	0.021			

[a]Energy required for removing unit volume of material.

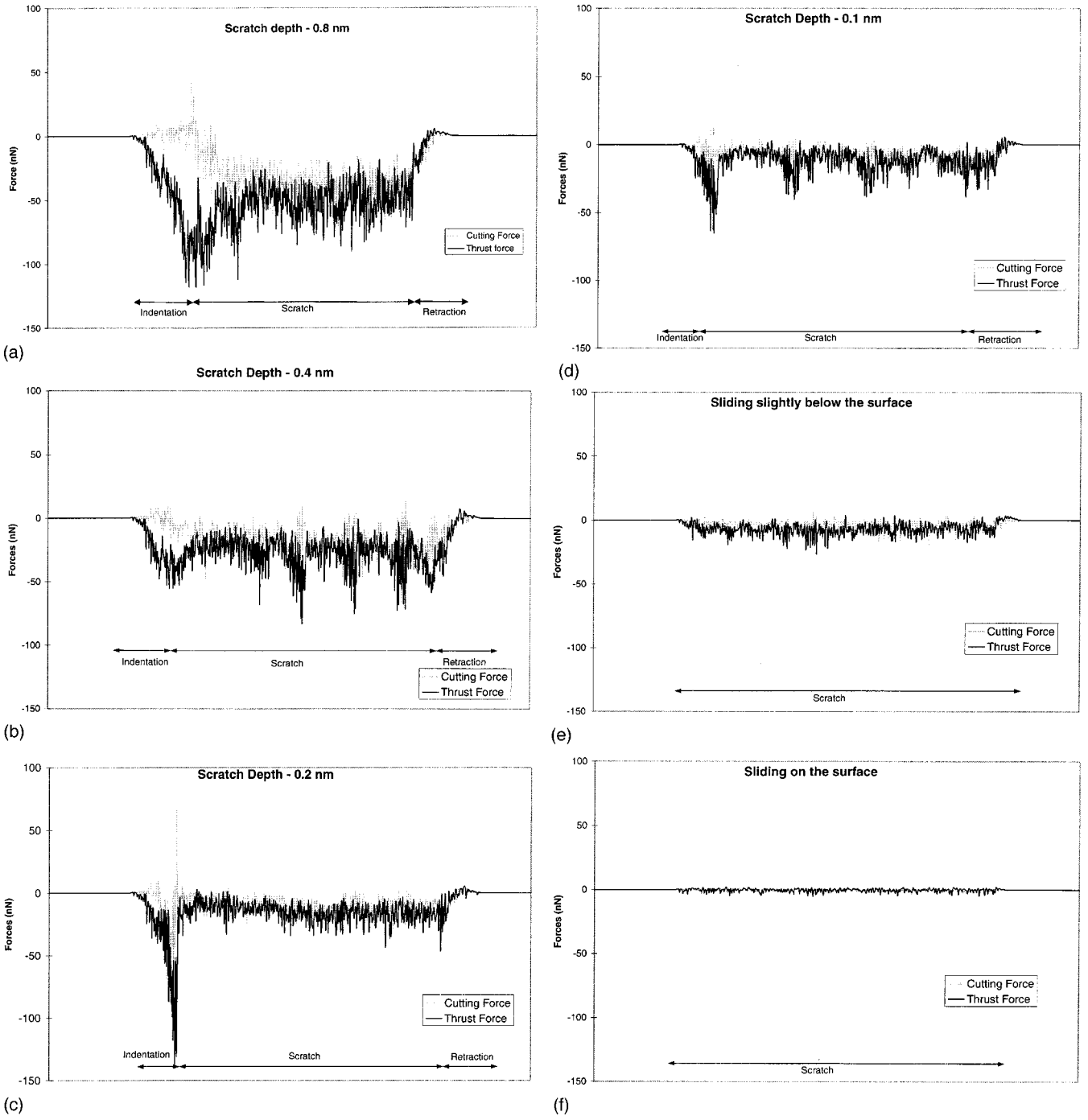

FIG. 8. Force-displacement plots obtained in MD simulation of indentation/scratching at various depths (a) 0.8 nm, (b) 0.4 nm, (c) 0.2 nm, (d) 0.1 nm, (e) sliding slightly below the surface, and (f) sliding on the surface.

rameter by $\pm 5\%$. It can be seen that the scratch force, the normal force, and the resultant force decrease with decreasing D parameter. However, the variation is within the experimental error limits. As the D parameter is reduced, with the other parameters remaining constant, the well depth of the Morse potential curve decreases. This results in a reduction in the force required to deform the atomic bonds. Consequently, both the scratch and the normal forces decrease with decreasing D parameter. The reverse holds true when the D parameter is increased resulting in an increase in the forces. However, the data in Table IV show that when the D parameter is varied by $\pm 5\%$, the corresponding friction coefficient values vary by $<1\%$.

V. DISCUSSION

It can be seen from Fig. 9(b) that the friction coefficient is independent of the depth of sliding and the values of friction coefficient are significantly high (~ 0.6). This is attributed to the tool (slider) presenting a high negative rake angle of $-45°$ during sliding. It may be noted that the 90° indenter used in the present investigation is considered as a sharp indenter in the indentation field, which in fact is a blunt tool in cutting with a $-45°$ rake. Other pyramidal or conical indenters with higher included angles as well as spherical indenters present even higher negative rake angles. Marshall and Shaw[54] reported the mean grinding coefficient, which is

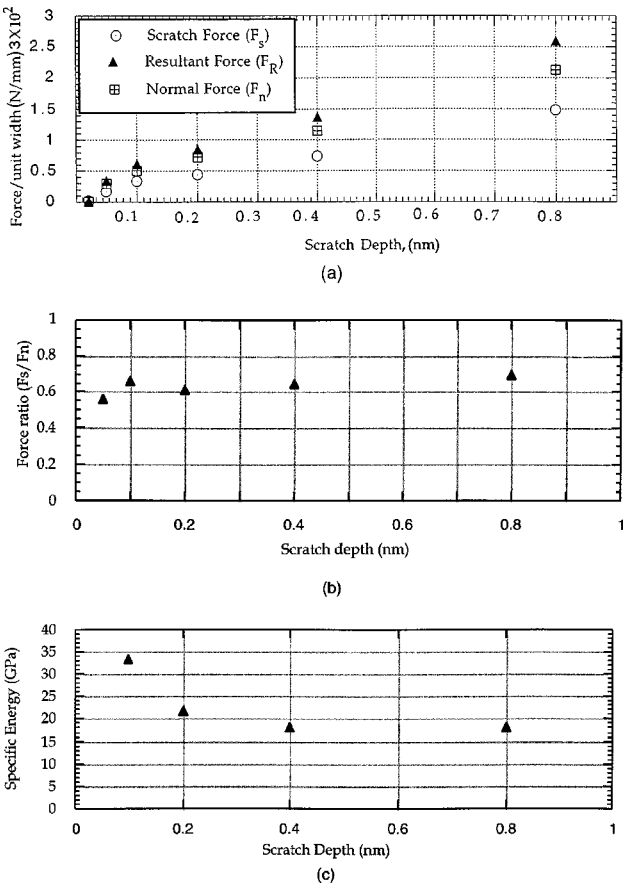

FIG. 9. Variation of (a) the scratching force, the normal force, the resultant force, (b) the friction coefficient, and (c) the specific energy during the scratch process for various scratch depths (0.8 nm to almost 0).

the ratio of the cutting force to thrust force for grinding with a silicon carbide wheel, to be 0.47. In an earlier MD simulation study, on the effect of tool rake angle (over a wide range from 0° to −75°) on the ratio of forces, Komanduri, Chandrasekaran, and Raff[50] reported the ratio of the cutting to the thrust force for a −45° rake tool to be 0.58. Table V gives the ratios of the cutting to the thrust force for various rake angles from 0 to −75°. It can be seen that as the rake angle decreases from 0° to −75°, the ratio also decreases from 1.17 to 0.424, showing a strong effect of this ratio on the rake angle. In a subsequent study on the effect of tool geometry in nanometric cutting, Komanduri, Chandrasekaran, and Raff[55] carried out MD simulations by varying the tool edge radius r (3.62–21.72 nm) and depths of cut d (0.362–2.172 nm) by maintaining the d/r ratio constant (0.1, 0.2, and 0.3). They reported the ratio of the cutting (or

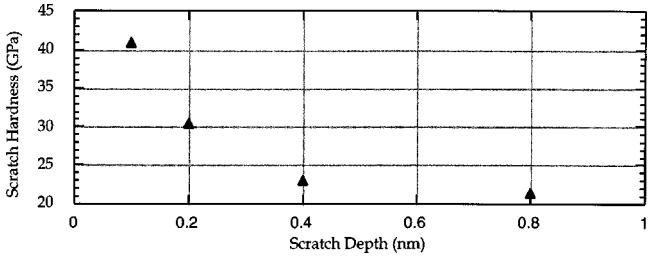

FIG. 10. Variation of scratch hardness with scratch depth.

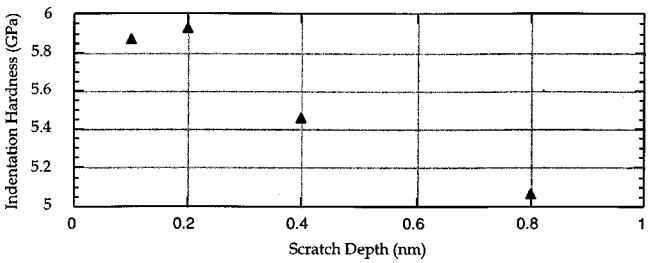

FIG. 11. Variation of indentation hardness with depth of indentation.

scratch, in this case) to the thrust (or normal) force to be in the range of 0.5–0.8 due to the high effective negative rake presented by the tool edge radius relative to the depth of cut. Based on the results of the simulations presented here, it can be seen that the friction coefficient values are in close agreement with those reported in the literature. Since the rake angle remains constant even with decreasing depths during the scratch process, the resulting ratio of the scratch force to the normal force (friction coefficient) should be nearly constant as found in this investigation.

Based on the sensitivity analysis, it is observed that the forces exhibit small variations as the D parameter of the Morse potential is varied. This is attributed to the variation in the material properties with changes in the Morse potential parameters. However, the friction coefficient varied only by a maximum of 1% as the D parameter was varied by ±5%. This suggests that the results obtained in this investigation are insensitive to variations in the Morse potential parameter within the experimental error percentage (±5%). The results also support the claim that the friction coefficient is highly dependent on the tool geometry and it remains constant even with small variations in material properties.

It can be noted from the review of literature that a wide range of friction coefficient values were reported from extremely low (0.005–0.015)[6,7,33] to extremely high (Garzino-Demo and Lama[28] reported a friction coefficient value of 1.2 and Shimizu *et al.*[29] reported maximum friction coefficient value of ~19). In one of the simulations conducted in the present investigation with the indenter just sliding on the surface (without material removal) of the work material, the friction coefficient was found to be somewhat high (2.1) (see Table III). However, based on the force values reported in Table III as well as the raw force data [Fig. 8(f)], it can be seen that the magnitude of the forces are extremely low and close to zero. Hence, it is possible that in sliding friction processes where the slider moves on the surface without material removal, the forces can be extremely low and very close to zero. However, when the slider is moving on the surface at a finite depth, in addition to the molecular interactions, mechanical contact and subsequent damage of the substrate are possible.[27] Under such conditions, it is not appropriate to assume that sliding experiments are nondestructive. A similar situation exists when measuring the surface finish with a stylus type of instrument, especially on soft materials (e.g., aluminum and copper used in optical mirrors). One can clearly observe the scratches made by the stylus with a sensitive instrument. Use of a noncontact surface finish measuring instrument, such as an optical interference contrast microscope, is the only alternate to measure surface roughness.

TABLE IV. Results of MD simulation study on the stability of Morse potential by varying the D parameter.

Variation of D parameter	Scratch force/ unit width (F_s) 10^2 (N/mm)	Normal force/ unit width (F_n) 10^2 (N/mm)	Resultant force /unit width (F_R) 10^2 (N/mm)	Friction coefficient (F_s/F_n)
0.2703	0.337	0.510	0.611	0.661
0.2568(−5%)	0.310	0.465	0.559	0.667
0.2838(+5%)	0.348	0.525	0.630	0.663

Indeed, the nature of scratching by a stylus-type instrument has to be reevaluated in terms of elastic and plastic deformation of a blunt indenter at extremely light loads.

When the sliding process is destructive resulting in permanent deformation of the substrate, it very much resembles the atomic-scale scratching process. In such a case, the forces are defined by the tool nomenclature in addition to various other factors (depth of sliding, work material properties, etc.). Even when sliding is performed at a few atomic layers depth, the tip of an AFM or STM presents a high effective negative rake angle similar to a spherical indenter. Consequently, based on this study, it is proposed that as long as the rake angle of the tool plays a significant role in the scratch process, the friction coefficient will be a measure of the force ratio. However, when the slider slides on the surface without any material removal and the rake angle effect is insignificant, the friction coefficient depends on a number of other factors including the accuracy of the instrumentation used to measure forces and the surface state. Unless the surface is covered by a lubricant, it is unlikely that the friction coefficient would be low, as some researchers reported earlier. For example, Mate *et al.*[6] and Erlandsson *et al.*[7] reported friction coefficient values in the range of 0.005–0.015. However, their experiments were conducted in ambient air. It is possible that the surfaces may have been covered with a monolayer of a weak film that may have acted as a lubricant. In such cases, sliding involves breaking of weak van der Waal bonds as opposed to the much stronger metallic bonds that we represent with a Morse potential that can result in very low friction coefficient values. In the case of MD simulations, the surfaces are atomically smooth and totally free of any contaminant.

Both the indentation and scratch hardness were observed to increase with decreasing depth. It may be noted that the calculated hardness values are an order of magnitude higher than the engineering values obtained at a macro level as was observed earlier by other research workers.[38,43] This can be attributed to the fact that as the experimentation scale decreases, the plastic deformation is governed by the theoretical yield strength of the material. Belak, Boercker, and Stowers.[38] reported a hardness of 5.4 GPa for a silver substrate based on their MD simulations. This is close to the theoretical hardness value of 4.5 GPa. They also proposed a similar rationale for the high hardness values.

TABLE V. Variation of the force ratio for various rake angles (Ref. 50).

Rake angle (degrees)	Force ratio (cutting/thrust)
0	1.170
−15	0.922
−30	0.714
−45	0.579
−60	0.526
−75	0.424

VI. CONCLUSIONS

MD simulations of indentation/scratching were performed on single crystal aluminum at extremely low depths (0–0.8 nm) to investigate atomic-scale friction, such as the variation of friction coefficient and hardness with scratch/indentation depth. The following are some of the specific conclusions that may be drawn based on this investigation.

(1) The ratio of scratch force to the normal force (friction coefficient) was observed to be significantly high (~0.6) and independent of the normal force on the indenter in the nano-Newton range. One reason for the higher friction coefficient values is that in MD simulations, the surfaces are totally free from any contaminant.

(2) The friction coefficient was found to be constant and independent of scratch depth except when the indenter was slid on the surface of the crystal without any material removal (zero scratch depth). This indicates that when material removal is involved in atomic-scale friction, the friction coefficient is dependent of the rake angle presented by the indenter and does not depend either on the scratch depth or the normal force.

(3) That the friction coefficient is independent of the normal force in atomic-scale friction involving material removal can be explained on the basis of large negative rake angle presented by the indenter during sliding. As the scratch depth increases, the normal force also increases, but the friction coefficient remains nearly constant due to constant rake angle.

(4) In an earlier MD simulation study on the effect of tool rake angle, Komanduri, Chandrasekaran, and Raff[50] reported the ratio of cutting to thrust force for a −45° rake tool to be 0.58, which is close to the friction coefficient value of 0.6 with a 90° indenter reported here.

(5) Both the indentation and scratch hardness values are found to increase with decreasing depth strongly suggesting a size effect.

(6) A sensivity analysis was conducted for one depth of scratch (0.1 nm) by varying the most important of the Morse parameters, namely, the D-parameter by ±5%. The resultant variation in the friction coefficient is observed to be <1%. The results are, therefore, rather insensitive to small variations in the model interaction potential.

(7) Based on the MD simulation results, it appears that the

low values of friction coefficient reported in the literature are possible only when the surfaces are covered with a lubricant. In such cases sliding involves breaking of weak van der Waal bonds that can result in very low friction coefficient values. Extrinsic factors such as surface contaminants, load, environment, etc., may affect the friction coefficient values in addition to molecular interactions between the contacting surfaces.

ACKNOWLEDGMENTS

This project was sponsored by grants from the Manufacturing Processes and Machines Program (DMI-9523551) of the Division of the Design, Manufacture, and Industrial Innovation (DMII) and the Tribology and Surface Engineering Program (CMS 9414610) of the Division of Civil and Mechanical Structures of the National Science Foundation. The authors thank Dr. Ming Leu, Dr. Delcie Durham, and Dr. B. M. Kramer of DMII and J. Larsen Basse of the Tribology and Surface Engineering Program for their interest in and support of this work. One of the authors (R. K.) also thanks the MOST Chair (Most Eminent Scholars Program) for enabling the preparation of the manuscript. The authors also thank Dr. Ali Noori-Khajavi for assistance with the initial simulation work, Mr. P. R. Mukund for assistance with some of the MD simulations, and Robert Stewart for help with the animation.

*FAX: (405) 744-7873.
Electronic address:ranga@ceat.okstate.edu

[1] S. M. Forehand and B. Bhushan, Tribol. Trans. **40**, 549 (1997).
[2] B. Bhushan, *Handbook of Micro/Nano Tribology*, (CRC Press, Boca Raton, FL, 1999).
[3] B. Bhushan, J. N. Israelachvill, and U. Landman, Nature (London) **374**, 607 (1975).
[4] R. Kaneko, Wear **168**, 1 (1993).
[5] R. Kaneko, S. Umemura, M. Hirano, Y. Andoh, T. Miyamoto, and S. Fukui, Wear **200**, 296 (1996).
[6] C. M. Mate, G. M. McClelland, R. Erlandsson, and S. Chiang, Phys. Rev. Lett. **59**, 1942 (1987).
[7] R. Erlandsson, G. Hadziioannou, C. M. Mate, G. M. McClelland, and S. Chiang, J. Chem. Phys. **89**, 5190 (1988).
[8] C. A. Coulomb, Mem. Math. Phys. Acad. Royale **10**, 161 (1785).
[9] F. P. Bowden and D. Tabor, *The Friction and Lubrication of Solids (Part I)* (Clarendon, Oxford, 1954).
[10] F. P. Bowden and D. Tabor, *The Friction and Lubrication of Solids (Part II)* (Clarendon, Oxford, 1964).
[11] N. P. Suh, Wear **25**, 111 (1973).
[12] G. A. Tomlinson, Philos. Mag. **7**, 905 (1929).
[13] Y. Mori, K. Endo, K. Yamamoto, H. Wang, and T. Ide, Int. J. Jpn. Soc. Precis. Eng. **56**, 679 (1980) (in Japanese).
[14] G. M. McClelland, in *Adhesion and Friction*, edited by M. Grunge and H. J. Kreuger Springer Series in Surface Sciences, Vol. 17 (Springer-Verlag, Berlin, 1989), p. 1.
[15] M. Cieplak, E. D. Elizabeth, and M. O. Robbins, Science **265**, 1209 (1994).
[16] B. N. J. Persson, Phys. Rev. B **50**, 4771 (1994).
[17] H. I. You and C. S. Yu, J. Chin. Soc. Mech. Eng. **18**, 371 (1997).
[18] G. A. Garzino and F. L. Lama, Surf. Coat. Technol. **86–87**, 603 (1996).
[19] S. C. Lim, M. F. Ashby, and J. H. Brunton, Acta Metall. **37**, 767 (1989).
[20] E. Rabinowicz, Wear **159**, 89 (1992).
[21] T. Tsukizoe and T. Sakamoto, Bull. JSME **18**, 65 (1975).
[22] Y. Enomoto and D. Tabor, Proc. R. Soc. London, Ser. A **373**, 405 (1981).
[23] M. Casey and J. Wilks, J. Phys. D **6**, 1772 (1973).
[24] F. U. Hillebrecht, M.Sc. thesis, Oxford University, 1981.
[25] J. Krim, Sci. Am. (Int. Ed.) **275** (4), 74 (1996).
[26] M. O. A. Mokhtar, Wear **78**, 297 (1982).
[27] D. E. Kim and N. P. Suh, Wear **149**, 199 (1991).
[28] G. A. Garzino-Demo and F. L. Lama, Surf. Coat. Technol. **76–77**, 487 (1995).
[29] J. Shimizu, H. Eda, M. Yoritsune, and E. Ohmura, Nanotechnology **9**, 118 (1998).
[30] G. Binnig, H. Rohrer, Ch. Gerber, and E. Weibel, Phys. Rev. Lett. **49**, 57 (1982).
[31] J. Skinner, N. Gane, and D. Tabor, Nature (London), Phys. Sci. **232**, 195 (1971).
[32] W. G. Hoover, A. J. De Groot, C. G. Hoover, I. F. Stowers, T. Kawai, B. L. Holian, T. Boku, S. Ihara, and J. Belak, Phys. Rev. A **42**, 5844 (1990).
[33] U. Landman, W. D. Leudtke, N. A. Burnham, and R. J. Colton, Science **248**, 454 (1990).
[34] U. Landman, W. D. Luedtke, and E. M. Ringer, Wear **153**, 3 (1992).
[35] U. Landman and W. D. Luedtke, Appl. Surf. Sci. **92**, 237 (1996).
[36] O. Tomagnini, F. Ercolessi, and E. Tosatti, Surf. Sci. **287/288**, 1041 (1993).
[37] W. Yan and K. Komvopoulos, J. Tribol. **120**, 385 (1998).
[38] J. Belak, D. B. Boercker, and I. F. Stowers, MRS Bull. **18**, 55 (1993).
[39] N. Chandrasekaran, A. Noori-Khajavi, L. M. Raff, and R. Komanduri, Philos. Mag. B **77**, 7 (1998).
[40] D. E. Kim and N. P. Suh, J. Tribol. **116**, 225 (1994).
[41] U. Landman, W. D. Luedtke, and M. W. Ribarsky, J. Vac. Sci. Technol. A **7**, 2829 (1989).
[42] A. Buldum and S. Ciraci, Phys. Rev. B **57**, 2468 (1998).
[43] R. Komanduri, N. Chandrasekaran, and L. M. Raff, Wear (to be published).
[44] R. Komanduri, N. Chandrasekaran, and L. M. Raff, Wear (to be published).
[45] R. W. Hertzberg, *Deformation and Fracture Mechanics of Engineering Materials*, 4th ed. (Wiley, New York, 1996).
[46] T. Inamura and N. Takezawa, Ann. CIRP **41/1**, 121 (1992).
[47] M. E. Riley, M. E. Coltran, and D. J. Diestler, J. Chem. Phys. **88/9**, 5934 (1988).
[48] L. A. Girifalco and V. G. Weizer, Phys. Rev. **114**, 687 (1959).
[49] R. Stewart, M.S. thesis, Oklahoma State University, 1998.
[50] R. Komanduri, N. Chandrasekaran, and L. M. Raff, Philos. Mag. B **79/7**, 955 (1999).
[51] Y. Furukawa and N. Moronuki, Ann. CIRP **37/1**, 113 (1988).
[52] K. Nakayama and K. Tamura, J. Eng. Ind. **90**, 119 (1968).
[53] D. A. Lucca, R. L. Rhorer, and R. Komanduri, Ann. CIRP **40/1**, 69 (1991).
[54] E. R. Marshall and M. C. Shaw, Trans. ASME **74**, 51 (1952).
[55] R. Komanduri, N. Chandrasekaran, and L. M. Raff, Wear **219**, 84 (1998).